

Operating Deflection Shapes from Continuous-Scan LDV measurements using Time Synchronous Averaging

Mahdi Mohammadi, Sebastian Oberst & Ben Halkon

Centre for Audio, Acoustics and Vibration, Faculty of Engineering & IT, UTS, 15 Broadway, Ultimo, NSW 2007, Australia

ABSTRACT

Conventional Continuous-Scan Laser Doppler Vibrometry (CSLDV) methods for Operational Deflection Shape (ODS) extraction such as lifting and polynomial techniques rely on frequency-domain processing through Fast Fourier Transform (FFT) and analysis of spectral sideband peaks. These approaches face limitations under high noise conditions – including making measurements from vibrating platforms – where elevated noise floors prevent effective sideband identification. This paper presents a novel time-domain methodology that directly reconstructs ODSs from raw CSLDV signals, eliminating the need for manual spectral processing. After synchronising the scanning mirror galvanometers in the CSLDV to the vibrating frequency of the target, a kernel-based framework employing Gaussian weighted averaging is used to reduce the signal noise through inherent Time Synchronous Averaging properties. Experimental validation including under multi-axis shaker platform vibration confirms successful ODS reconstruction in noise and vibration degraded environments. For the first bending mode of vibration for a simple cantilever beam, agreement between the recovered ODS and an analytical model achieved a mean Modal Assurance Criterion (MAC) of 0.986 ± 0.007.

1 INTRODUCTION

Continuous-Scan Laser Doppler Vibrometry (CSLDV) offers a non-contact way to rapidly assess structural vibrations by sweeping a probe laser beam over the target surface using a pair of orthogonal galvanometer mirrors (Halkon and Rothberg, 2018). Compared to single-point contacting vibration sensors such as accelerometers, a CSLDV system remotely captures vibration data along custom paths; these can be one-dimensional – i.e. a line scan, or two-dimensional – such as rectangular, circular, or conical scans (Stanbridge and Ewins, 1999). This enables sequential measurements across the surface of an object without requiring additional hardware, manual adjustments, or repositioning of the instrument. This makes it especially useful for inspecting large or intricate structures, especially in areas such as infrastructure health monitoring, aerospace, and automotive engineering, where the CSLDV helps identify structural or material defects, analyse fatigue, and analyse dynamic behaviour (Huang and Zang, 2019).

A key component here is the Operating Deflection Shape (ODS), which defines a structural vibrational response for a particular frequency of excitation. ODSs and mode shapes play a vital role in modal testing by illustrating real-world vibration shapes, supporting model validation, and pinpointing vibrational problems. Established methods for extracting ODS from CSLDV data are frequency domain-based using approaches like lifting or polynomial fitting (Di Maio et al., 2021). Lifting is a frequency-domain filtering technique used to isolate and analyse specific components of the measured CSLDV signal, which characteristically include a peak at the vibration frequency with sidebands separated by multiples of the scan frequency. A 'lifter' filter is applied to the spectrum of the CSLDV signal to primarily pass through the primary and sideband frequencies while rejecting the carrier and noise related content. The filtered spectrum then undergoes a complex procedure where it is demodulated, processed using an inverse FFT and mapped to reconstruct the ODS (Di Maio et al., 2021).

The polynomial fitting method treats the ODS as a series of mathematical functions, more specifically Chebyshev polynomials (Stanbridge and Ewins, 1999). The amplitudes of the central carrier frequency and corresponding sideband pairs are then extracted from the FFT. These extracted values are used as direct coefficients for the polynomial series to reconstruct the entire ODS (Castellini et al., 2016). Both the lifting and polynomial techniques

perform well in controlled laboratory setups, but they struggle in real-world applications, including those where the sensor head undergoes base motion vibration (Darwish et al., 2022), to which the measurement system is sensitive. In such cases higher noise and vibration levels – due to the base motion itself and due to that caused by the laser speckle effect (Rothberg et al., 2016) – can obscure sidebands which can prevent effective ODS extraction.

This reliance on clean FFTs and sideband spotting limits CSLDV application in noisy, practical, real-world settings where alternative reliable, automated tools are needed for effective measurement interpretation. To tackle this challenge, this paper presents a novel time-domain based approach to construct ODSs directly from unprocessed CSLDV signals, skipping the frequency domain steps altogether. It uses a kernel framework with Gaussian-weighted averaging where the scan frequency is synchronised to the target vibration frequency. Drawing on Time Synchronous Averaging (TSA) (Mohammadi et al., 2024), it removes noise via phase-cycling to reduce non-synchronous noise such as sensor head vibration. Core steps involve converting mirror angles to actual beam positions with the tangent function for geometry fixes, then applying kernel regression for even deflection estimates.

2 CLSDV DURING BASE MOTION VIBRATION

2.1 CSLDV Experimental Arrangement

CSLDV measurements, conducted from a Multi-Axis Simulation Table (MAST), were made from the vibration of an aluminium Rectangular-Hollow-Section (RHS) of 1 m length, as shown schematically in Figure 1 and as an annotated photograph of the actual set-up in Figure 2. The RHS beam was set up in a fixed-free configuration with the lower end of the beam clamped securely between two heavy steel plates. The clamped end was 0.2 m in length, with the free end of the beam thereby having a total length of 0.8 m. The beam was excited near to its base using a miniature electro-dynamic shaker with integrated amplifier (TMS K2004E01). The shaker was mounted to the railed walkway of the MAST and driven using a GW Instek multi-channel function generator (MGF-2260MFA). It was connected to the back surface of the RHS beam with an axially stiff pushrod.

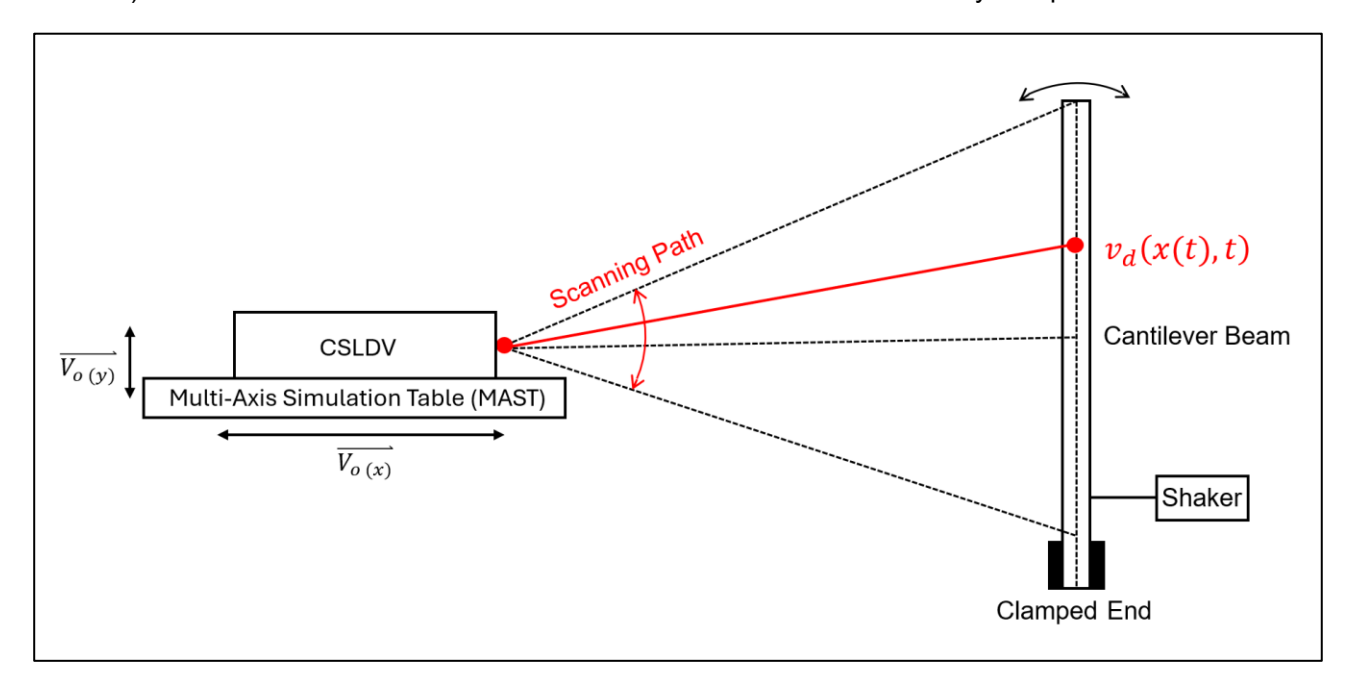


Figure 1: CSLDV Setup on Multi-Axial Simulation Table

Three DC-response 'Correction Accelerometers' (Endevco 770F-010-U-120) were fitted to the MAST, each orientated to capture the vibration of the MAST platform in the *x*-, *y*-, and *z*- directions, as shown in Figure 2. The locations and sensitive axes are deliberately aligned with the laser beam incidence on the second '*y* mirror' (vertical direction), enabling full compensation (in post-processing) of the measurement for arbitrary 6-DoF vibration of the sensor head (Halkon and Rothberg, 2021. The LDV (Polytec NLV-2500-5 Compact Laser Vibrometer) was fixed to a bespoke scanning assembly containing an orthogonal pair of galvanometer-controlled mirrors (Halkon and Chapman, 2018). The LDV and scanning assembly were mounted securely onto the MAST using a custom fixture, as can be seen in Figure 2. A Siemens Digital Industries Software SCADAS Mobile data acquisition system was used to acquire signals from the LDV and galvanometers with the internal, 2-channel Source Control

Page 2 of 9 ACOUSTICS 2025

waveform generator function used to provide the signals to drive the motor-controlled mirror(s) in the bespoke scanning laser Doppler vibrometry assembly.

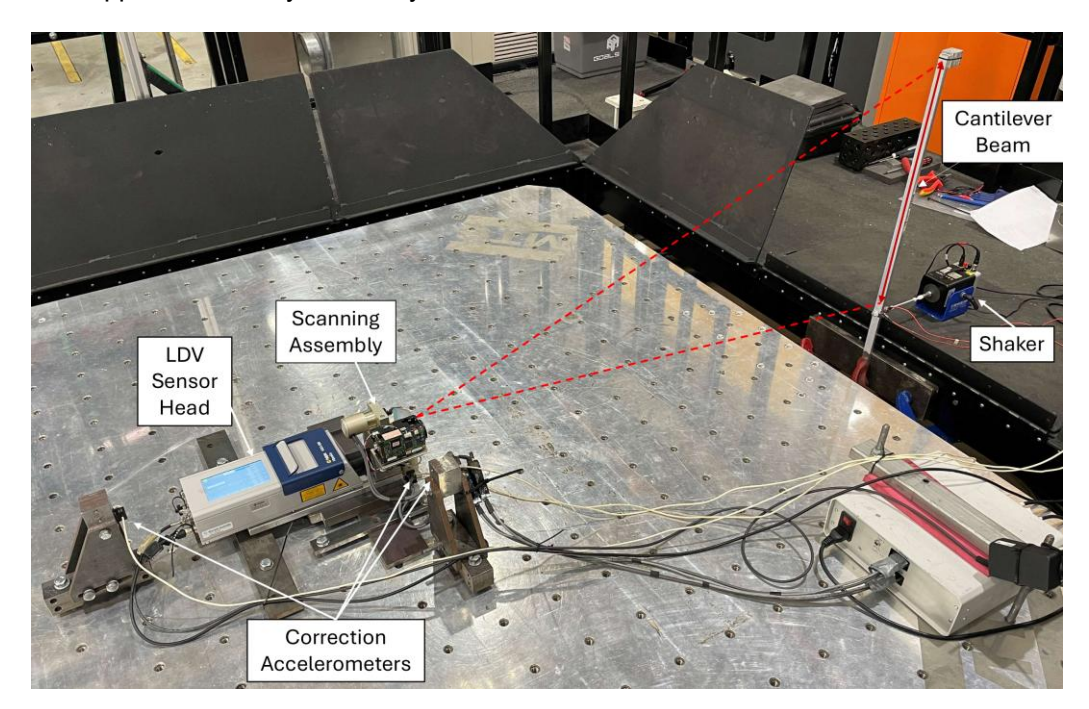


Figure 2: Experimental CSLDV setup on the MAST (a MTS 354.20 Square Table 6-DoF hexapod)

2.2 Conventional ODS post-processing

To demonstrate the challenges associated with sensor head vibration in CSLDV signals, a measurement campaign was conducted as per the setup previously described, with the cantilever beam excited at (approximately) its first resonant frequency of 9 Hz while the CSLDV scan rate was set to 4 Hz. The measurement was repeated several times with the MAST both stationary and vibrating the CSLDV sensor head in combinations of DoFs during testing. The effects of sensor head vibration in the time-domain can be seen in Figure 3 below.

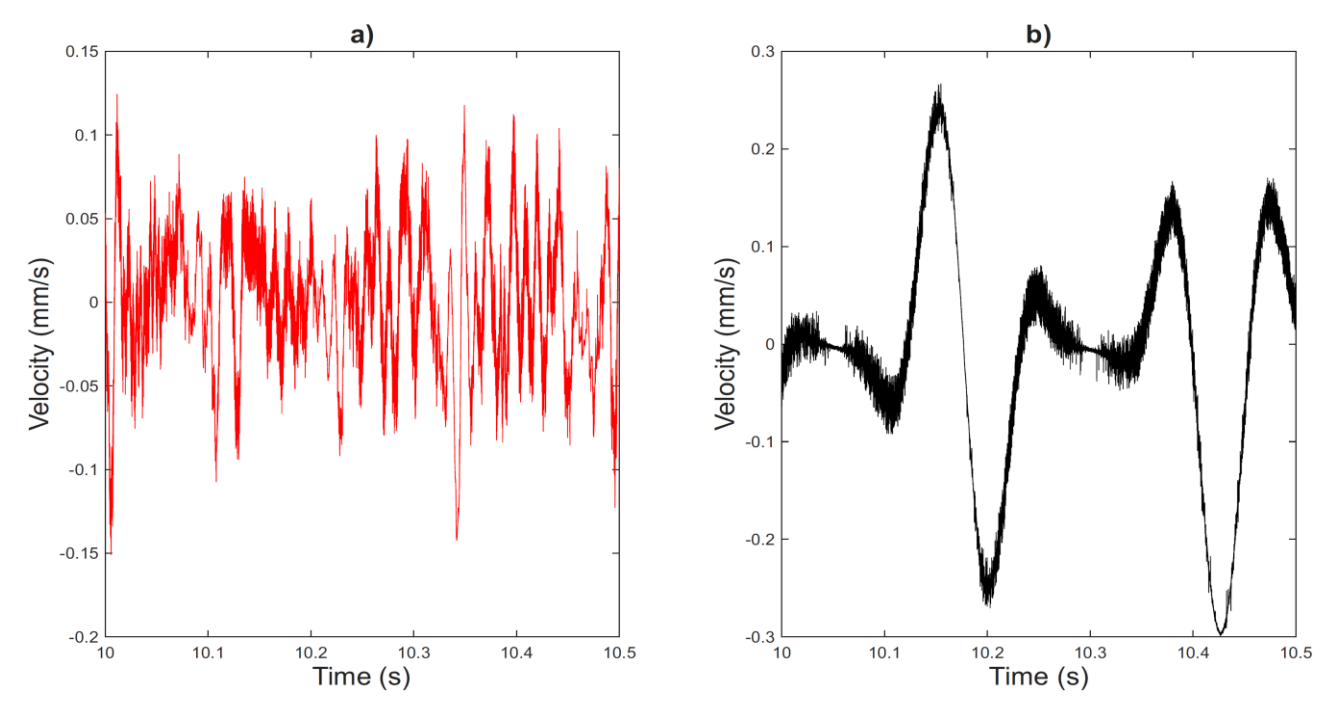


Figure 3: CLSDV measurement with (a) and without (b) sensor head vibration

ACOUSTICS 2025 Page 3 of 9

The detrimental effects of the base motion on the time-domain signal are clearly illustrated in Figure 3(a) where the otherwise underlying periodic structure of the signal is contaminated by high amplitude, non-synchronous noise that prevents interpretation of the beam true velocity profile. This is in contrast to Figure 3(b) which presents the cleaner (reference) signal acquired without sensor head vibration in which the smooth, periodic velocity profile resulting from the periodic scanning of the laser across the vibrating beam is more clearly defined. Despite the inevitable noise due to the laser speckle effect which is also present on the signal, one complete line scan from root back to root can be seen in Figure 3(b) from ~10.05 to ~10.3 s. The effects of the base motion vibration and the differences between the two signals in Figure 3(a) and (b) are even more pronounced when presented in the frequency domain, as shown in Figure 4 below.

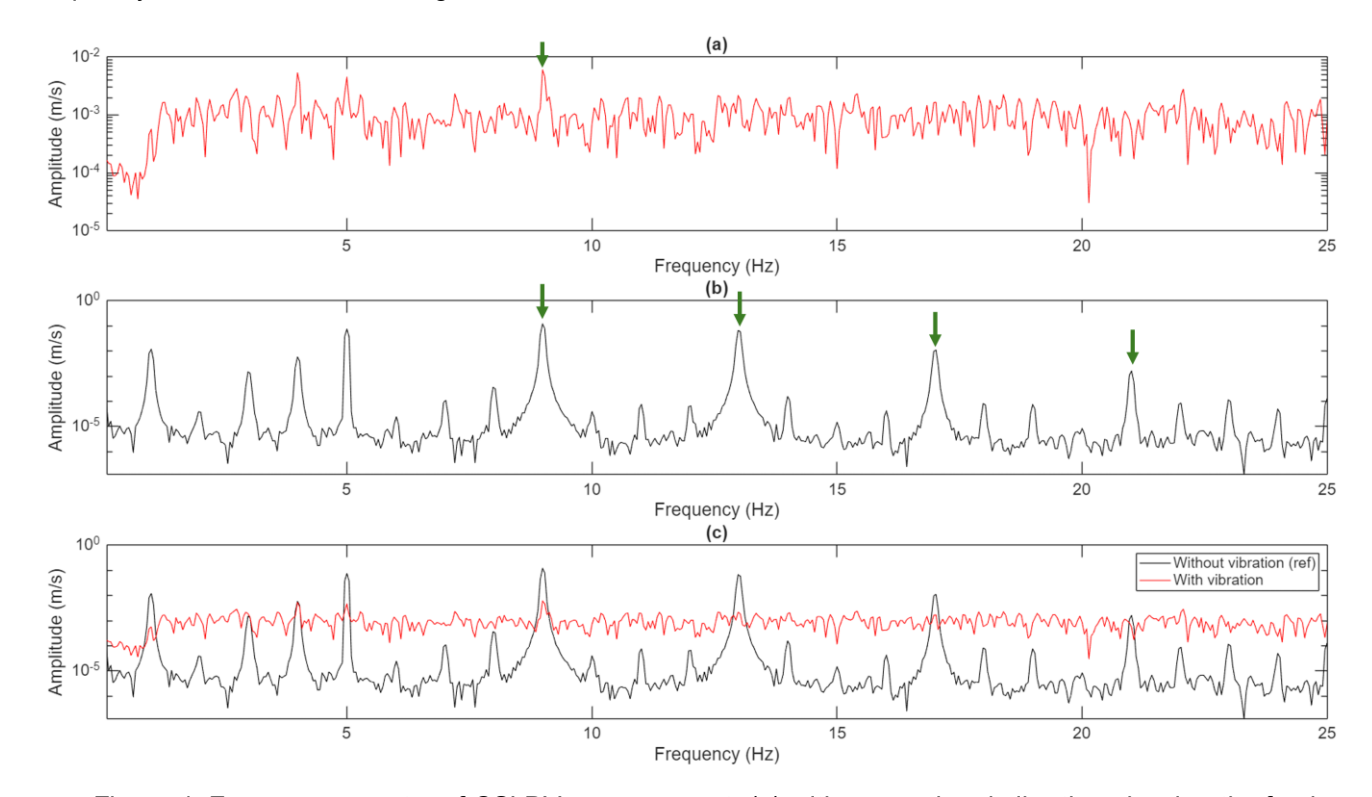


Figure 4: Frequency spectra of CSLDV measurement: (a) with sensor head vibration showing the fundamental beam vibration frequency (at 9 Hz) marked with a green arrow, (b) reference measurement without sensor head vibration, showing lower noise floor and clearly identifiable sidebands at the vibration frequency plus integer multiples of the scan frequency (at 13 Hz, 17 Hz, 21 Hz), and (c) signals overlaid for direct comparison.

In Figure 4(a), sensor head vibration results in an elevated noise floor across all frequencies with this increased noise floor obscuring the critical sideband harmonics that are necessary for traditional ODS extraction using the polynomial method. Only the fundamental frequency of the beam at 9 Hz is readily identifiable. In contrast, the reference measurement without sensor head vibration shown in Figure 4(b) exhibit a significantly lower noise floor with clearly identifiable sidebands. These distinct peaks as indicated by green arrows contain the crucial spatial information for frequency-domain reconstruction of the ODS.

Once the identified fundamental frequency and sidebands are extracted from each spectrum, the ODS can be calculated using the polynomial method as seen in Figure 5 (Di Maio, 2021). For the noisy signal and given the associated inability to identify any sidebands, the ODS developed was a flat, zero-amplitude line, as seen in Figure 5(a). This occurs because, with only the fundamental frequency and no sidebands, the polynomial method has no spatial information to process the ODS. Meanwhile for the reference CSLDV measurement and given the clearly identifiable sidebands from the spectrum, the polynomial method can be used to successfully reconstruct the expected ODS for a cantilever beam first bending mode, as shown in Figure 5(b).

Page 4 of 9 ACOUSTICS 2025

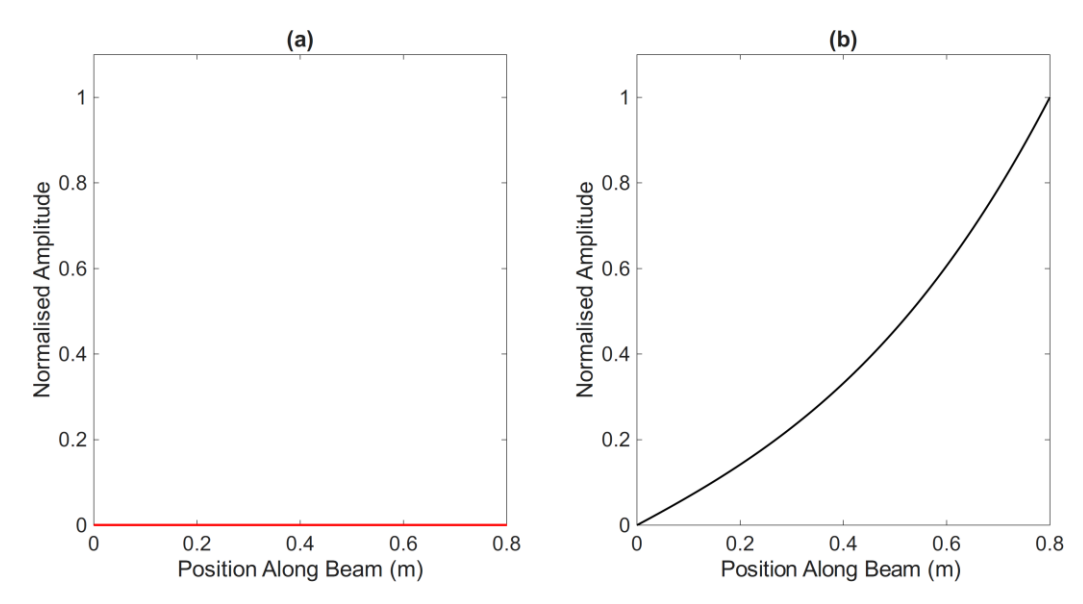


Figure 5: Reconstructed ODS using the polynomial method: (a) with, and (b) without sensor head vibration

3 PROPOSED METHODOLOGY FOR TSA-BASED DIRECT ODS RECOVERY

3.1 Theoretical Formulation

For a linear, time-invariant structure subject to a sinusoidal excitation at frequency ω_e , the steady state response at point x can be expressed as the following (Rothberg et al. 2016):

$$v_d(x,t) = V_r(x)\cos(\omega_e t) + V_i(x)\sin(\omega_e t) \tag{1}$$

where V_r and V_i are the in-phase and quadrature components of the vibration measurement. Given that in a continuous scanning setup the laser spot scans the target surface via a pair of orthogonal galvanometer mirrors, point x can be redefined to x(t), (Rothberg and Tirabassi, 2013) where x(t) is the time-varying position of the laser beam determined by the galvanometer scan frequency ω_s (typically sinusoidal scanning). Based on Eq (1), the measurement signal from the LDV can be expressed as follows:

$$y(t) = V_r(x(t))\cos(\omega_e t) + V_i(x(t))\sin(\omega_e t) + n(t)$$
(2)

where y(t) is the observed LDV measurement and n(t) is the noise present in the signal, including electronic noise, speckle noise and sensor head vibrations. The measurement signal can then be rectified:

$$|y(t)| = |V_r(x(t))\cos(\omega_e t) + V_i(x(t))\sin(\omega_e t) + n(t)|$$
(3)

with this step required as direct time-domain averaging of the raw vibration signal, y(t), would otherwise converge towards zero for the vibration signal over a large number of cycles, as the symmetric positive and negative oscillations would cancel out, leaving only noise artefacts. By only taking the absolute value, the signal is folded to be all positive, preserving the vibration envelope for further processing to ultimately extract the ODS. The expression $V_r(x(t))\cos(\omega_e t) + V_i(x(t))\sin(\omega_e t)$ can be simplified to $V_d(x)\cos(\omega_e t - \phi(x))$, where taking the time average over the period $T_e = 2\pi/\omega_e$ yields:

$$\frac{1}{T_e} \int_0^{T_e} |v_d(x(t), t)| \cdot dt = V_D(x) \cdot \frac{1}{T_e} \int_0^{T_e} |\cos(\omega_e t - \phi(x))| dt = V_D(x) \cdot \frac{2}{\pi}$$

$$\tag{4}$$

Eq (4) implies that by averaging the rectified velocity measurements over a sufficiently large number of vibration cycles, the ODS magnitude can be directly recovered, scaled by $\frac{2}{\pi}$.

3.2 Scan Frequency and Phase Cycling

The scan frequency, $f_s = \omega_s/(2\pi)$ is set to be slightly offset from the excitation frequency, $f_e = \omega_e/(2\pi)$, according to the following relationship:

ACOUSTICS 2025 Page 5 of 9

$$f_s = f_e \left(1 + \frac{1}{n} \right) \tag{5}$$

where n is an integer. This intentional frequency mismatch creates a slow beat (assuming high n values) between scan and excitation frequencies, enabling phase cycling, incrementally shifting the phase relationship between the vibration and the laser beam position over subsequent scans. Over n excitation cycles, the phase at each spatial point advances by 2π radians, sampling the point at n discrete phase angles that are uniformly distributed between 0 and 2π . A higher n values reduces the frequency offset between excitation and scan frequency, resulting in slower phase progression and finer resolution over the phase space. However, this comes at a clear tradeoff: higher n values require longer measurement times to complete the full measurement.

By applying the averaging process over a total of M scan cycles in the measurement, an approximation of $\hat{y}(x)$ can be expressed as the sum of the structural component and the averaged noise component:

$$\hat{y}(x) \approx \frac{2}{\pi} V_d(x) + \frac{1}{M} \sum_{m=1}^{M} n(t)$$
 (6)

While $V_d(x)$ is constructively recovered and preserved through the synchronised averaging process, the stochastic, non-deterministic noise signal n(t) is averaged towards zero with increasing M. Here, M represents the number of full phase cycle periods being averaged over. If the measurement contains a total of N_{total} vibration cycles (excitation cycles), then $M = \frac{N_{total}}{n}$.

3.3 ODS Reconstruction using TSA

The time-averaged data points must be mapped to their corresponding spatial locations and smoothed to form a continuous ODS. This is achieved using a spatially weighted average of the velocity measurements. The reconstruction procedure follows these steps:

i. Geometric Correction

The galvanometer feedback angles θ_i (in degrees) are converted to linear positions along the beam p_i , to correct for angular distortion. Assuming near-perpendicular incidence and a stand-off distance D:

$$p_i = D \cdot tan\left(\theta_i \cdot \frac{\pi}{180}\right) \tag{7}$$

ii. Grid Discretisation

The surface is discretised to a set of n_{points} uniformly distributed points, $p_c(j)$ across the target (scan region).

iii. Kernel Weighting

A Gaussian kernel is used to calculate weights, w_{ii} , based on the distance between each raw data position p_i and each evaluation point $p_c(j)$. The kernel bandwidth, h, determines the degree of smoothing:

$$w_{ii} = \exp\left(-\frac{(p_i - p_c(j))^2}{2h^2}\right)$$
 (8)

iv. Kernel Averaging

The weights for each point are then normalized and used to calculate the ODS estimate, $\hat{y}(p_c(j))$, from the absolute LDV measurements, $y_i = |LDV_i|$.

$$\hat{y}(p_c(j)) = \frac{\sum_{i=1}^{N} w_{ii} y_i}{\sum_{i=1}^{N} w_{ii}}$$
(9)

v. Baseline Correction

The DC bias from the signal is removed $\hat{y}(p_c(j)) = \hat{y}(p_c(j)) - \hat{y}(p_c(1))$. This ensures the first point, which is the clamped end of the structure, to be set as the zero-deflection reference. This may change if different configurations are used (i.e., in a fixed-fixed configuration, both ends would be set to zero). The final output of this procedure $\hat{y}(p_c(j))$ produces the estimated ODS of the cantilever beam. A visual guide to this process is illustrated in Figure 6.

Page 6 of 9 ACOUSTICS 2025

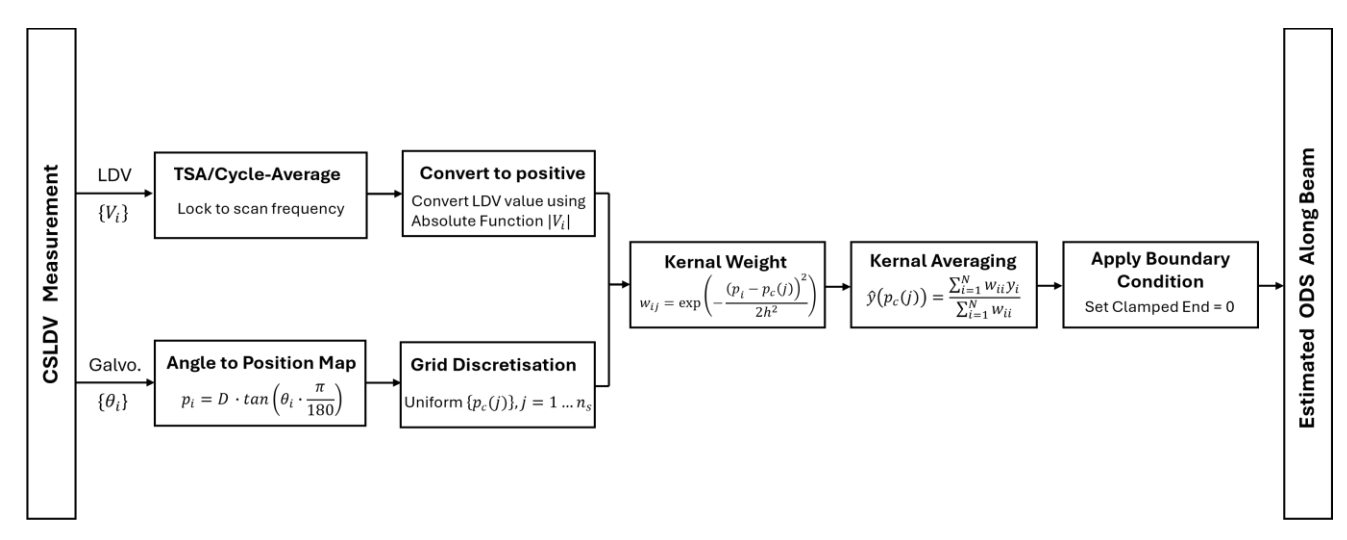


Figure 6: Proposed method to capture ODS

4 RESULTS

4.1 Analytical Reference Model

An analytical mode shape for a uniform cantilever beam was derived using Euler-Bernoulli beam theory to provide a theoretical benchmark. Clamped-free boundary conditions applied to the free-vibration governing equation produce the transcendental characteristic equation defining discrete wavenumbers β_n (Farokhi et al., 2022):

$$\cosh(\beta L)\cosh(\beta L) + 1 = 0 \tag{10}$$

The first non-zero root – for the fundamental bending mode – is $\beta_n L \approx 1.875104$, yielding the mode shape $\phi_A(x)$, as the reference to evaluate the effectiveness of the proposed methodology:

$$\phi_A(x) = (\cosh(\beta_1 x) - \cos(\beta_1 x) - \sigma_1 \sinh(\beta_1 x) - \sin(\beta_1 x))$$
(11)

Where the mode shape constant σ_1 is given by:

$$\sigma_1 = \frac{\cosh(\beta_1 L) + \cos(\beta_1 L)}{\sinh(\beta_1 L) + \sin(\beta_1 L)} \tag{12}$$

4.2 Experimental ODS Validation

ODS extractions were performed in accordance with the described approach for experiments exciting the beam at (approximately) its first natural frequency (9 Hz). While the ODS at 9 Hz does not equate directly to the first mode shape, given that the beam was carefully excited at close to its first resonant frequency, the response of the beam will align closely with that mode, making the ODS a close proxy for the theoretical shape and enabling valid correlation.

A visual comparison of the extracted shapes is presented in Figure 7, which shows a strong qualitative agreement with the analytical model. For a more robust quantitative assessment, the measured ODS (ϕ_E) was directly compared to the analytical mode shape (ϕ_A) . The correlation was performed using the Modal Assurance Criterion (MAC), which measures the collinearity between the two eigenvectors and can be expressed as the following expression (Huang and Zang 2019):

$$MAC = \frac{|\phi_A^h \phi_E|^2}{(\phi_A^h \phi_A)(\phi_E^h \phi_E)}$$
 (13)

Where h denotes the transposed conjugate vector. The MAC values were calculated for the experimental datasets, achieving a mean MAC value of 0.986 ± 0.007 . This high average MAC value confirms that the extracted ODS is a highly accurate representation of the expected structural motion and that, therefore, the proposed approach to extract the ODS directly from the time-domain data using TSA is reasonable, even in the presence of significant additional measurement signal content due to the arbitrary vibration of the CLSDV sensor head.

ACOUSTICS 2025 Page 7 of 9

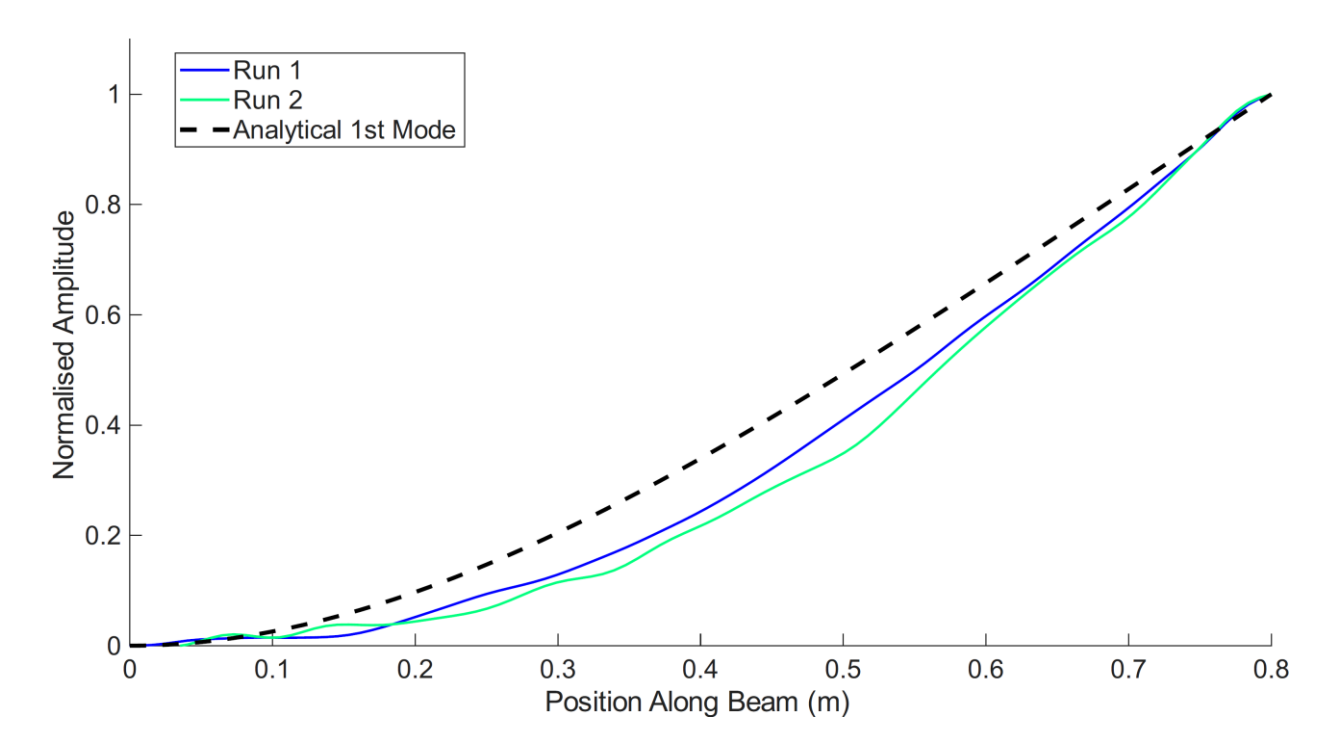


Figure 7: Comparison between experimentally derived ODS and the normalised analytical first mode shape of the cantilever beam

5 CONCLUSIONS

This paper introduces a novel time-domain methodology for extracting Operating Deflection Shapes (ODS) directly from Continuous-Scan Laser Doppler Vibrometry (CSLDV) data. By synchronising the laser scan frequency with the target vibration and leveraging the noise-reducing principles of Time Synchronous Averaging through a kernel-based framework, the approach bypasses the limitations of conventional frequency-domain techniques. The primary contribution is the development of a robust ODS extraction method that remains effective in noisy conditions where traditional methods, which are reliant on clear spectral sidebands, would normally fail. Experimental validation on a cantilever beam under significant sensor-head vibration confirmed the method efficacy, achieving a mean Modal Assurance Criterion (MAC) of 0.986 ± 0.007 when compared to an analytical model. This shift from delicate frequency analysis to robust time-domain averaging marks a significant step towards enabling reliable CSLDV measurements in more challenging, real-world applications where background interference and instrument vibration are unavoidable. However, validation of the approach was conducted for a simple cantilever beam excited at a single, known resonant frequency. Future research should therefore focus on expanding the method applicability by testing it on more complex structures and ODSs, by developing an adaptive algorithm that can handle broadband, transient, or unknown excitations. Successfully addressing these areas would further establish this time-domain approach as a standard, highly reliable tool for in-situ vibration-based structural health monitoring.

REFERENCES

Castellini, P., et al. 2016. 'Re-sampling of continuous scanning LDV data for ODS extraction'. *Mechanical Systems and Signal Processing* 72-73 (5): 667-677. doi:10.1016/j.ymssp.2015.10.035.

Darwish, A., et al. 2022. 'A comparison of time and frequency domain-based approaches to laser Doppler vibrometer instrument vibration correction'. *Journal of Sound and Vibration* 520 (3): 1160607. doi:10.1016/j.jsv.2021.116607.

Di Maio, D., et al. 2021. 'Continuous Scanning Laser Vibrometry: A raison d'être and applications to vibration measurements'. *Mechanical Systems and Signal Processing* 156 (7): 107573. doi:10.1016/j.ymssp.2020.107573.

Farokhi, H., et al. 2022. 'Experimentally validated geometrically exact model for extreme nonlinear motions of cantilevers'. *Nonlinear Dynamics* 107 (1): 457-475. doi:10.1007/s11071-021-07023-9.

Page 8 of 9 ACOUSTICS 2025

Proceedings of ACOUSTICS 2025 12-14 November 2025, Joondalup, Australia

- Halkon, B. and C. Chapman 2018. 'On the development and characterisation of a synchronised-scanning laser Doppler vibrometer system.' In *Proceedings of the 25th International Congress on Sound and Vibration 2018 (ICSV25*): 2876–2883. Hiroshima, Japan.
- Halkon, B.J. and S.J. Rothberg 2017. 'Reprint of: Taking laser Doppler vibrometry off the tripod: correction of measurements affected by instrument vibration'. *Optics and Lasers in Engineering* 99 (12): 3-10. doi:org/10.1016/j.optlaseng.2017.08.003.
- Halkon, B.J. and S.J. Rothberg 2018. 'Towards laser Doppler vibrometry from unmanned aerial vehicles'. *Journal of Physics: Conference Series* 1149 (1): 012022. doi:10.1088/1742-6596/1149/1/012022.
- Halkon, B.J. and S.J. Rothberg 2021. 'Establishing correction solutions for scanning laser Doppler vibrometer measurements affected by sensor head vibration'. *Mechanical Systems and Signal Processing* 150 (3): 107255. doi:10.1016/j.ymssp.2020.107255.
- Huang, Z. and C. Zang 2019. 'Damage Detection Using Modal Rotational Mode Shapes Obtained with a Uniform Rate CSLDV Measurement'. *Applied Sciences* 9 (23): 4982. doi:10.3390/app9234982.
- Mohammadi, M., et al. 2024. 'Application of Time Synchronous Averaging in Mitigating UAV Noise and Signal Loss for Continuous Scanning Laser Doppler Vibrometry." *Journal of Physics: Conference Series* 2698: 012005. doi: 10.1088/1742-6596/2698/1/012005.
- Rothberg, S., et al. 2016. 'An international review of laser Doppler vibrometry: Making light work of vibration measurement'. *Optics and Lasers in Engineering* 99 (12): 11-22. doi:10.1016/j.optlaseng.2016.10.023.
- Rothberg, S. J. and M. Tirabassi 2013. 'Development of a scanning head for laser Doppler vibrometry (LDV) using dual optical wedges'. *Review of Scientific Instruments* 84 (12): 121704. doi:10.1063/1.4845555.
- Stanbridge, A. B. and D. J. Ewins 1999. 'Modal testing using a scanning laser Doppler vibrometer'. *Mechanical Systems and Signal Processing* 13 (2): 255-270. doi:10.1006/mssp.1998.1209.

ACOUSTICS 2025 Page 9 of 9